

Molecule-Dependent Quantum Yield in Photon Emission Scanning Tunneling Microscopy of Mixed Amphiphile Monolayers on Au(111)

G. E. Poirier^{*,†}

Chemical Science and Technology Laboratory, National Institute of Standards and Technology, Gaithersburg, Maryland 20899
(Received 26 July 2000)

Contrast in photon yield between phase-separated domains of reduced and photo-oxidized alkanethiols comprising a mixed molecular monolayer on Au(111) was observed using an ultrahigh vacuum scanning tunneling microscope. The photon quantum yield of the two surface species was measured to be independent of tunneling gap width, within experimental uncertainty, suggesting a novel photon emission mechanism. The spatial resolution of the photon maps was 20 nm. These results indicate that photons emitted by a scanning tunneling microscope reveal chemical information with nanometer spatial resolution on molecularly heterogeneous surfaces.

DOI: 10.1103/PhysRevLett.86.83

PACS numbers: 61.16.Ch, 79.60.-i

The question of whether chemically heterogeneous systems will generate contrast in simultaneously acquired photon maps has been addressed in recent literature. Alvarado *et al.* measured contrast in images of cross sections of GaAs/AlGaAs multiple quantum well structures [1]. Berndt *et al.* reported contrast for islands of C₆₀ on Au(110) [2]. Evoy *et al.* reported photon yield contrast between bare Au and Au covered with a monolayer of octadecanethiol [3]. Downes *et al.* reported contrast for Au and Ag clusters deposited on Si(111) (7 × 7) [4] and also for silicon carbide clusters on Si(111) [5]. Thirstrup *et al.* reported contrast for the case of patterns of dangling bonds written on a hydrogen-terminated Si(100) surface [6], and Bottomley *et al.* reported contrast for nanometer-scale germanium phosphide dots on Ge(001) [7]. All of these prior studies demonstrated material-specific contrast in photon maps. In each case, the contrast was between two inorganic substances or between organic and inorganic surface regions. Evidence indicates that metal surfaces emit photons by a plasmon mediated process [8], and semiconductors emit photons by radiative carrier recombination [1]. It is possible that the material contrast observed to date is due to a disparity in cross section for the different emission processes occurring in mixed organic/inorganic or metal/semiconductor systems. One question that remains unanswered, and is relevant to the analysis of surfaces modified with organic or biomolecular films, is whether the scanning tunneling microscope excited electromagnetic field contains molecule-specific information.

In this Letter we demonstrate photon contrast for a surface comprising a heterogeneous distribution of dissimilar organic molecules. The system chosen for study is a surface mixture of reduced and oxidized alkanethiols, the structure of which is known from a prior study [9]. The paper begins with a description of the photon collecting apparatus. This is followed by a discussion of topographs and simultaneously acquired photon maps of the mixed alkanethiol monolayers. Measurements of the

tunneling-gap-width dependence on the photon quantum yield are then discussed, followed by a summary.

Studies were conducted on a single crystal Au(111) surface in an ultrahigh vacuum (UHV) chamber. Scanning tunneling microscopy (STM) data were acquired using a custom-built instrument operated at a constant tunneling current between 10 and 4000 pA and tunneling bias between ±0.5 and 2.2 V. The Au(111) single crystal was cleaned by Ar⁺ sputtering at 500 eV, 2 μA, and subsequent annealing at 500–600 °C for 10 min. Monolayers were prepared by placing the clean Au(111) crystal in a glass incubation dish, covering with 3–4 ml of 1 mM decanethiol solution, and incubating overnight (12 to 14 h). Partial oxidation of the monolayer was achieved by exposing to either ozone or a combination of oxygen and UV light [9]. The photon collecting apparatus was mounted on a 2.75 in. conflat flange on our UHV STM. The detector was a commercially available avalanche biased silicon photodiode with integral control electronics. The total efficiency of the photon collecting apparatus was roughly 0.01.

Figure 1(A) shows a nascent decanethiolate monolayer. The monolayer is characterized by a mosaic of commensurate crystalline domains [10–12] separated by a molecular-width domain boundary network [13] that itself is decorated by Au vacancy islands [14]. Figure 1(B) shows the decanethiolate monolayer following exposure to nominally pure ozone for 4 min [9]. Evidence indicates that ozone reacts specifically with the thiol headgroups [9,15], converting them to sulfonates or sulfonates [15,16], and that the hydrocarbon section of the molecule remains intact [9,15]. The monolayer shown in Fig. 2(B) is characterized by separate domains of thiolate, a striped phase, and a disordered phase. The striped phase is attributed to partially oxidized thiols; the disordered phase is attributed to fully oxidized thiols [9]. The oxidation state of molecules comprising the striped phase is unknown; however, for the purpose of this discussion we refer to all nonthiolate domains as sulfonate.

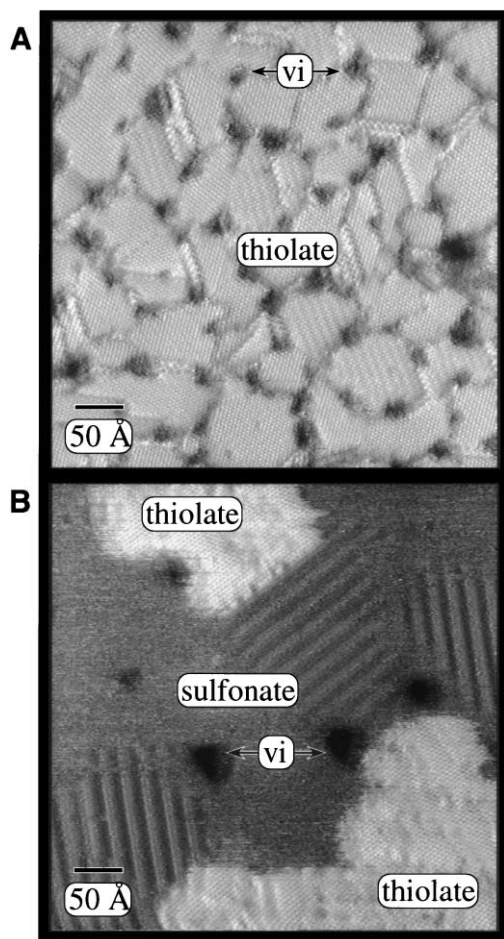


FIG. 1. Constant-current STM topographs of decanethiol monolayer and partially oxidized decanethiol monolayer. (A) Nascent decanethiolate monolayer comprising domains of crystalline, commensurate Au thiolates separated by a domain boundary network. Dark features are Au vacancy islands, two of which are indicated by black arrows (vi). (B) Partially oxidized monolayer comprising thiolate domains with nominally the same crystalline packing structure as (A) (thiolate) and domains of a fluid and a striped phase of oxidized thiols (sulfonate).

Topographs and simultaneous photon maps were measured on this two-component monolayer. For the data shown in Fig. 2, the monolayer was photo-oxidized *in situ* for 30 min. The structural and chemical evolution of monolayers undergoing photo-oxidation is similar to that for ozone oxidation [9,15]. Figure 2(A) shows a topograph of a partially photo-oxidized monolayer. As in Fig. 2(B), we assign the light areas in Fig. 2(A) to thiolate domains and the dark areas to sulfonate domains. Figure 3(C) shows the cross-sectional profile from the line trace indicated by the white arrow in Fig. 2(A). Thiolate and sulfonate domains are vertically displaced by ≈ 1 Å. Because the sulfonate domains are disordered, we have no evidence for the chain orientation in these domains. This step may be topographic in origin, arising from a difference in molecular areal density between sulfonate and thiolate regions, or it may be electronic, arising from withdrawal

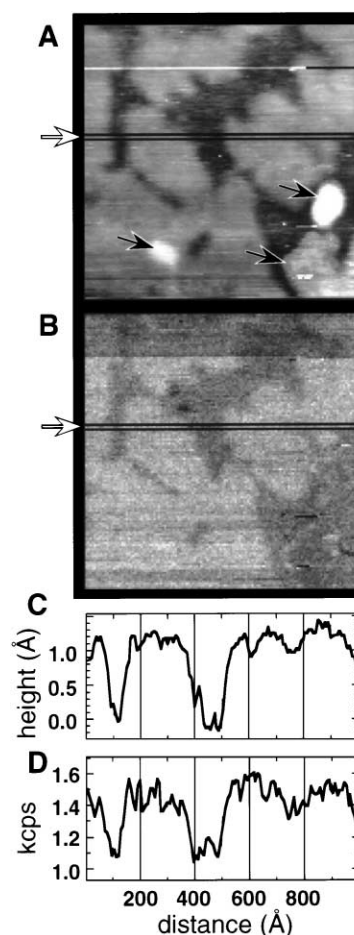


FIG. 2. Simultaneously acquired STM topograph and photon map of partially oxidized alkanethiol monolayer. Both images are 128×128 pixels, acquisition time was 30 min, tunneling current was 200 pA, and tunneling bias was 2.0 V. (A) Constant current topograph. Light regions are thiolate; dark regions are sulfonate; black arrows indicate topographic features without photon contrast. (B) Photon map acquired at 100 ms photon integration time. Contrast correlates with phase-segregated thiolate and sulfonate domains in (A). (C) Cross-sectional profile of the line trace indicated by white arrow in (A) quantifies tip displacement between molecular domains. (D) Cross-sectional profile of the line trace indicated by white arrow in (B), after subtracting dark counts, quantifies molecular contrast.

of electron density from the Fermi level by the oxidized headgroups in the sulfonate domains, or it may be a combination of these.

Figure 2(B) shows a photon map that was acquired pixelwise simultaneous to the topograph shown in Fig. 2(A). Shorter integration times were not feasible under these tunneling conditions because the number of counts would then have approached the dark count noise. Higher tunneling current set points or tunneling bias voltages were likewise not feasible because this resulted in unstable tunneling and modification of the monolayer structure. Molecular resolution was not obtained at the tunneling parameters required to generate a detectable photon emission rate. Contrast in Fig. 2(B) is spatially correlated with topographic features

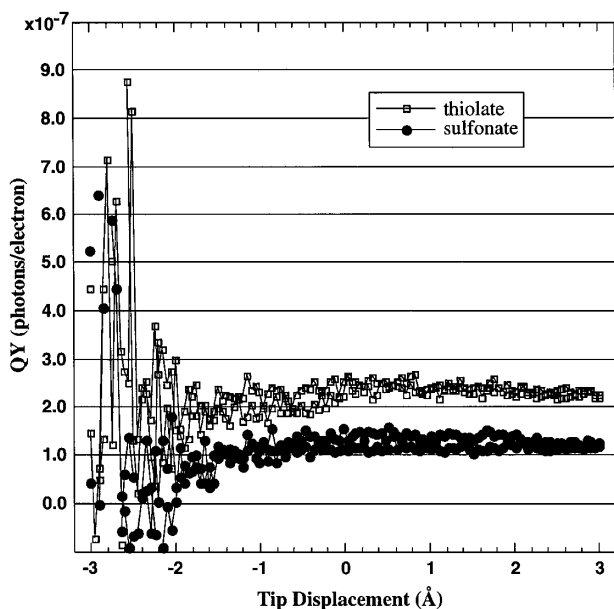


FIG. 3. Variation of photon quantum yield with tip-sample distance at constant tunneling bias voltage acquired over a thiolate domain (open squares) and a sulfonate domain (filled circles). The forward- and backward-going scans are nearly indistinguishable, indicating negligible positional hysteresis. Zero tip displacement corresponds to the tunneling gap determined by tunneling parameters prior to breaking the feedback loop; positive tip displacement corresponds to decreasing gap width. Thiolate domains exhibit higher quantum yield than sulfonate; neither domain exhibits tunneling-gap-width dependence of photon quantum yield, within experimental uncertainty.

in Fig. 2(A). In Fig. 2(A) there are several surface protrusions indicated by black arrows. The leftmost and uppermost protrusions exhibit no contrast in the corresponding region of the photon map, Fig. 2(B). The lowermost feature exhibits only edge highlight in the photon map. These features are therefore most likely topographical in origin, rather than chemical. The contrast between thiolate and sulfonate regions is quantified in the cross-sectional profile, Fig. 2(D). Correcting for the dark count rate, the thiolate regions exhibit $\approx 35\%$ higher photon yield than the sulfonate regions.

Before attributing the observed contrast to molecule-dependent quantum yield, we have to consider artifacts. For example, the observed contrast could be due to a tunneling-gap-dependent photon quantum yield; that is, it could be an artifact of the topographic step height. To determine if this is the case, the tunneling-gap dependence of the photon quantum yield (QY) was measured separately over thiolate and sulfonate regions. In these measurements, the STM feedback loop is interrupted, the tip retracted 3 \AA at constant tunneling voltage, the tip is then advanced 6 \AA during which the tunneling current is measured, the tip is then retracted 6 \AA again measuring the tunneling current, and finally the tip is advanced 3 \AA to its starting point whereupon feedback is reestablished. This

measurement provides current-distance curves and reveals positional hysteresis. The measurement was repeated 6 times; each measurement required $\approx 1 \text{ s}$. The detection channel was then changed from tunneling current to photon count and the measurement repeated 6 times; each measurement required $\approx 25 \text{ s}$. Both measurements were repeated over thiolate and sulfonate regions of the monolayer shown in Fig. 2. The QY is calculated by averaging the repetitions, then dividing the photon emission rate, corrected for the dark count rate, by the electron tunneling rate. The QY thus calculated accounts only for those photons that are detected. The lens system's efficiency, as discussed in the experimental section, is ≈ 0.01 ; therefore, the actual QYs are likely ≈ 100 times larger than the calculated values.

Prior studies in the literature have reported the dependence of photon quantum yield on the tunneling gap width. Berndt *et al.* reported a gain of $\approx 7\%$ per angstrom of approach for single-wavelength QY for a W tip over a Cu(111) surface [17]. This observation was explained by confinement-induced enhancement of the electromagnetic field strength of localized plasmon modes [8]. The electromagnetic field strength of tip-localized plasmon modes is largest in the vacuum and decays rapidly in the tip and the sample [17]. In related work, Berndt *et al.* observe the opposite trend for C_{60} on Au(110); molecule-resolved photon maps show a maximum in photon QY at topographical apices—points where the tip-substrate distance is greatest [18]. This they tentatively attribute to a novel mechanism whereby the molecules interact strongly with electromagnetic modes of the tip-sample cavity [18].

Downes *et al.* reported a loss of roughly 65% per angstrom of approach for all-wavelength QY for a W tip over a Si(111) (7×7) surface [5]. They argue that this is due to a crossover from plasmon-mediated to recombination-mediated luminescence in the reconstructed Si(111) surface. Si(111) (7×7) can be thought of as a 2 \AA thick metallic termination on a semiconducting bulk. The localized plasmon is supported only in this 2 \AA thick metallic surface layer and its magnitude is thought to decrease with decreasing gap width.

The results of our measurements are shown in Fig. 3. For tip withdrawal greater than 1.5 \AA (displacement between -1.5 and -3.0 \AA), the photon emission rates and electron tunneling rates both drop to a level where the quotient becomes dominated by noise. For tip displacements in the range -1 to $+3 \text{ \AA}$, relative to the set-point gap, the data are dominated by signal and do not reveal any dependence of photon quantum yield on tip-sample gap within experimental uncertainty. The measurement was repeated on a separately prepared sample and again showed a photon quantum yield with no statistically significant gap-width dependence. Any trend in the curves is less than the noise on the curves and cannot explain the observation of $\approx 35\%$ contrast between thiolate and sulfonate domains in Fig. 2(B). The evidence

therefore indicates that the contrast observed in Fig. 2(B) is not a gap-dependent artifact but rather arises from a photon-quantum yield that is dependent on molecular identity.

Our results show that, within our experimental uncertainty, the photon QY is independent of tunneling gap. This contradicts prior results and indicates that the photon emission mechanism for our system may be different than the plasmon-mediated case for metal-vacuum-metal junctions [17]. Berndt *et al.* tentatively suggest that the emitted electromagnetic field may be mediated by molecular adsorbates [18]; our results indicate a similar effect. Moreover, we find that the field is further mediated by the chemical identity of the molecular adsorbate.

One of the most important parameters in imaging-type chemical analysis techniques is the spatial resolution. From Fig. 1 we determine that the boundaries between thiolate and sulfonate domains are molecularly abrupt. The topographic step profiled in Fig. 2(C) extends over a distance of 20 Å, suggesting that these data were acquired with a tip whose radius was larger than that for Fig. 1. The photon step profiled in Fig. 2(D) extends over a distance comparable to that for the topograph, placing an upper limit on the photon map spatial resolution for this system at 20 Å. It is possible that better resolution could be obtained for images acquired with sharper tips and at higher pixel resolution than that for Fig. 2.

A phase-separated mixed amphiphile monolayer was characterized using photon emission STM. The photon quantum yield was measured to be nominally independent of tunneling gap width over a range of 4 Å, a range large enough to account for all observed topographic features. The results indicate that the local photon-quantum yield for this system is a function of molecular identity. This

study suggests that photon emission STM may be useful to discriminate between chemical species on molecularly heterogeneous surfaces with nanometer spatial resolution.

G. E. P. is grateful for helpful discussions with R. Berndt, A. Davies, D. T. Pierce, M. J. Tarlov, and D. J. Vanderah.

*Deceased.

†Address correspondence to Michael J. Tarlov.

Electronic address: michael.tarlov@nist.gov

- [1] S. F. Alvarado *et al.*, *J. Vac. Sci. Technol. B* **9**, 409 (1991).
- [2] R. Berndt *et al.*, *Appl. Phys. A* **57**, 513 (1993).
- [3] S. Evoy *et al.*, *J. Vac. Sci. Technol. A* **15**, 1438 (1997).
- [4] A. Downes and M. E. Welland, *Appl. Phys. Lett.* **72**, 2671 (1998).
- [5] A. Downes and M. E. Welland, *Phys. Rev. Lett.* **81**, 1857 (1998).
- [6] C. Thirstrup *et al.*, *Phys. Rev. Lett.* **82**, 1241 (1999).
- [7] D. J. Bottomley *et al.*, *J. Vac. Sci. Technol. A* **17**, 698 (1999).
- [8] R. Berndt and J. K. Gimzewski, *Ann. Phys. (Leipzig)* **2**, 133 (1993).
- [9] G. E. Poirier *et al.*, *J. Am. Chem. Soc.* **121**, 9703 (1999).
- [10] G. E. Poirier and M. J. Tarlov, *Langmuir* **10**, 2853 (1994).
- [11] E. Delamarche *et al.*, *Langmuir* **10**, 2869 (1994).
- [12] J.-P. Bucher, L. Santesson, and K. Kern, *Appl. Phys. A* **59**, 135 (1994).
- [13] G. E. Poirier, *Chem. Rev.* **97**, 1117 (1997).
- [14] G. E. Poirier, *Langmuir* **13**, 2019 (1997).
- [15] Y. Zhang, *J. Am. Chem. Soc.* **120**, 2654 (1998).
- [16] Y. Li *et al.*, *J. Am. Chem. Soc.* **114**, 2428 (1992).
- [17] R. Berndt, J. K. Gimzewski, and P. Johansson, *Phys. Rev. Lett.* **71**, 3493 (1993).
- [18] R. Berndt *et al.*, *Phys. Rev. Lett.* **74**, 102 (1995).